3J2-2

GHz surface-wave ultrasound tomography
GHz 弾性表面波を用いた超音波トモグラフィー

Hayato Takeda[1‡], Paul Otsuka[1], Motonobu Tomoda[1], Osamu Matsuda[1] and Oliver B. Wright[1] ([1] Faculty of Engineering, Hokkaido Univ.)
武田 颯[1‡], Paul Otsuka[1], 友田 基信[1], 松田 理[1], Oliver B. Wright[1] ([1] 北大工)

1. Introduction

There is a constant demand for non-destructive inspection methods that can image internal structure. Tomography is one performant method to meet this requirement. In tomographic imaging, one obtains a map of internal structure by scanning from outside a sample. This method has been applied in many fields, e.g. medical imaging [1] and material damage detection. [2]

In particular, ultrasound tomography reconstructs sound velocity and ultrasound attenuation. [3,4] Its spatial resolution depends is of the order of the wavelength of the applied ultrasound. With a GHz ultrasound source, the image has microscale resolution. However, there have been no reports of such techniques involving GHz ultrasound, owing to the difficulty of generating and detecting such a high frequency wave. Moreover, the higher attenuation of GHz ultrasound compared to lower frequencies is also an obstacle for measurement. Gigahertz surface acoustic wave propagation can be observed with the optical pump and probe technique, but this method has never been applied to ultrasound tomography.[5]

Here, we show by simulation how GHz ultrasonic pulses can be used to achieve surface wave ultrasound tomography.

2. Image Reconstruction method

Consider the situation where a scattering body is surrounded by a homogeneous isotropic medium as shown in **Fig. 1 (a)**. [3,4] Source wave excitation and scattered wave detection are performed on a circle of radius R that encloses the scattering body. We also assume that the scattering by the structure of the body is weak. Line sources with an acoustic wave vector $\boldsymbol{k_0} = (k\cos\theta, k\sin\theta)$ are used at variable angles θ, yielding corresponding elastically scattered wave components at wave vector $\boldsymbol{k} = (k\cos\phi, k\sin\phi)$. $\boldsymbol{k_0}$ and $\boldsymbol{k}$ have the same magnitude $k = \omega/c_0$, where ω is the frequency of the incident wave and c_0 is the longitudinal sound velocity of the surrounding medium. The complex amplitude $\psi_s(\theta,\phi)$ of each scattered component is recorded at angle ϕ ranging from $\theta - \frac{\pi}{2}$ to $\theta + \frac{\pi}{2}$, i.e for the forward scattering case. The acoustic profile $O(\boldsymbol{r})$ at position vector $\boldsymbol{r}$ is defined by

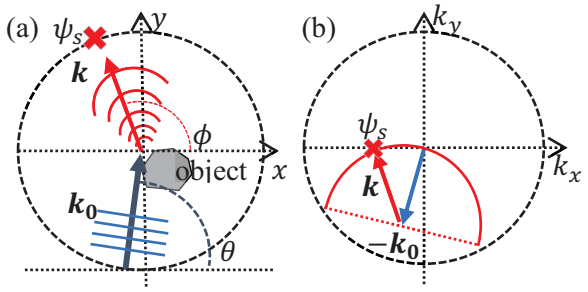

Fig. 1 Schematic diagram of the general geometry used. (a) Line source (blue) applied to the scattering object and scattering wave (red) is detected at, for example, the point marked by the cross. (b) Each measured value is plotted onto a corresponding point in k space.

$$O(\boldsymbol{r}) = 1 - \frac{c_0^2}{c(\boldsymbol{r})^2}, \tag{1}$$

where $c(\boldsymbol{r})$ is the sound velocity of the surrounding medium at position vector $\boldsymbol{r}$. By solving the wave equation [3], one finds

$$\tilde{O}[k(\cos\phi - \cos\theta), k(\sin\phi - \sin\theta)] = f(k,R)\psi_s(\theta,\phi). \tag{2}$$

Here, $\tilde{O}[\boldsymbol{k}]$ is the spatial Fourier transform of $O(\boldsymbol{r})$ and $f(k,R)$ is a factor which depends on wavenumber $k = |\boldsymbol{k_0}| (= |\boldsymbol{k}|)$ and R. **Fig. 1 (b)** shows a semicircle on which the measured value ψ_s is plotted for the example of the choice of $\boldsymbol{k_0}$ and $\boldsymbol{k}$ in Fig. 1(a). As θ is changed, this semicircle rotates in k space. When the incident angle θ and the detection angle ϕ are varied over all possible directions, the Fourier transform of $O(\boldsymbol{r})$ can be reconstructed from the measured values of ψ_s. The imaging process can therefore be completed with the following steps:

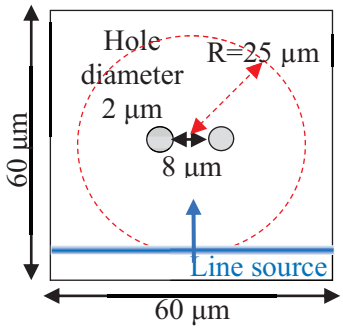

Fig. 2 Simulated geometry consisting of crown glass containing two holes of the same diameter 2 μm and same depth 1 μm. The excitation and detection are referred to the red dashed circle of radius R = 25 μm.

Email: htakeda@eng.hokudai.ac.jp

1. measure scattered waves for a line source at angle θ at scattered angles ϕ from $\theta - \frac{\pi}{2}$ to $\theta + \frac{\pi}{2}$;
2. repeat step 1 for all θ around the circle.
3. plot for each value ψ_s the corresponding point in k space calculated with Eq. (2);
4. take the inverse Fourier transform of $\tilde{O}[\boldsymbol{k}]$.

The reconstructed area in k space is a circle with radius $\sqrt{2}k$. Using the relation $k = 2\pi/\lambda$, where λ is the acoustic wavelength of the line source, the spatial resolution is given by

$$\left(\frac{\sqrt{2}k}{2\pi}\right)^{-1} = \frac{\lambda}{\sqrt{2}}. \qquad (3)$$

In the case of GHz surface acoustic waves, this value is of the order of a few μm.

3. Simulation

Simulations are conducted using the finite element method with the simulation software PZFlex, as shown in **Fig. 2**. The model involves a volume of 60×60×50 μm^3 containing the crown glass sample (of longitudinal sound velocity assumed to be 2800 m/s) . Two 2 μm diameter holes of depth 1 μm are included as a weak scattering structure. The holes are separated by a distance of 8 μm, as shown. The acoustic line source is 60 μm in length and 4 μm in width, in the form of a top-hat function and the spatial derivative of a Gaussian function, respectively. The latter dimension applies to the full-width-at-half maximum before taking the spatial derivative. The temporal variation of this source follows a ¼ of a sine period, a variation that lasts for 8.4 ps. The chosen circle radius is *R*=25 μm. The centers of the line sources, i.e. the excitation points, and the probe points are located every 2.5°, giving 72 probe points in total for each excitation point.

Since each line source contains broadband frequency components, we take the temporal Fourier transform of each detected wave and extract the frequency components. **Fig. 3 (a)-(c)** shows the reconstructed image of $|O(\boldsymbol{r})|$ at 1 GHz (λ = 2.8 μm), 700 MHz (λ = 4.0 μm), and 500 MHz (λ = 5.6 μm), respectively. Apart from the central artifact, the two holes are clearly resolved at 1 GHz and 700 MHz, whereas for 500 MHz the contrast is only just sufficient for their resolution. The image contrast can be better understood by means of the line profiles in **Fig. 4**. From Eq. (3), the spatial resolution is 2.0 μm for 1 GHz, 2.8 μm for 700 MHz and 4.0 μm for 500 MHz. Our results are in reasonable agreement with these predictions. Ring-shape phantoms are also evident in **Fig. 3**. We hope to minimized this effect with more sophisticated algorithms in future.

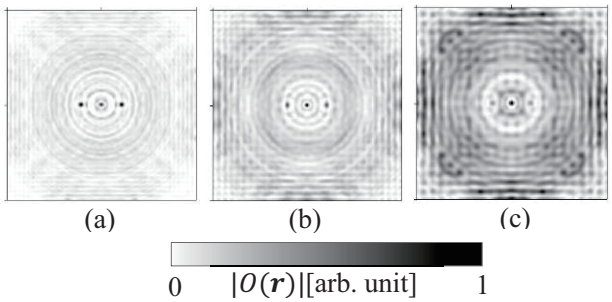

Fig. 3 Image of a 50×50 μm^2 region reconstructed at (a) 1 GHz, (b) 700 MHz and (c) 500 MHz. The colour represents the normalized absolute value of the acoustic profile $\boldsymbol{O}(\boldsymbol{r})$.

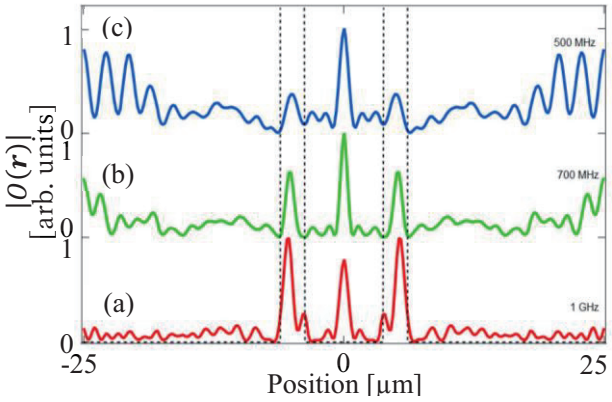

Fig. 4 Normalized line profiles of the reconstructed images shown in Fig. 3 (a)-(c) The black dotted lines show the edges of the 2 μm diameter holes.

4. Conclusions

We have demonstrated a new surface acoustic wave image reconstruction method based on ultrasound tomography theory at GHz frequencies. We obtained images with microscale resolution as expected. The GHz frequency range is experimentally accessible using the optical pump and probe technique, and we hope to verify the method in practice. In future, this method can be expanded to three-dimensional tomography to enable the mapping of internal structure with ~100 nm spatial resolution at ~100 GHz with laser-generated and detected longitudinal waves.

References

1. A. Cormack: J. Appl. Phys. **34** (1963) 2722.
2. V. Haach and F. Ramirez: Const. Build. Mat. **119** (2016) 61.
3. A. Devaney and G. Beylkin: Ultrason. Imag. **6** (1984) 181.
4. A. Kak and M. Slaney: *Principles of Computerized Tomographic Imaging* (IEEE Press,1988)
5. Y. Sugawara *et al.*: Phys. Rev. Lett. **88** (2002) 185504.